

EURO-COST

**DIRECTIONAL 3D REAL-TIME DUAL-POLARIZED MEASUREMENT OF
WIDEBAND MOBILE RADIO CHANNEL**

Abstract: This paper presents a measurement system for directional 3D real-time measurements of the wideband mobile radio channel. The system is based on a spherical antenna array and it enables the complete characterization of the mobile radio channel including time, delay, polarization, and direction in 3D. The measured signal statistics can be used e.g. for developing polarization or pattern diversity antennas for handheld devices.

Kimmo Kalliola

IRC/Radio Laboratory
Helsinki University of Technology
P.O.Box 3000, FIN-02015 HUT, Finland

Nokia Research Center
P.O.Box 407, FIN-00045 Nokia Group
Finland

**This paper will be presented also
in IMTC'99 in Venice, Italy**

1. Introduction

The demand for higher data rates sets high requirements for the future wireless communication systems. Efficient use of limited frequency spectrum requires thorough understanding of the behavior of the system, including the radio channel, that is the most difficult part to model. This understanding can be obtained either by prediction based on e.g. ray tracing simulations, or measurements of real channels. The former approach requires reliable simulation tools that, themselves, must be verified with measurement data.

The radio channel is a complex function of time, frequency, space, and direction. Therefore the directional real-time measurement of the channel is not an easy task. It requires simultaneous (or nearly simultaneous) reception of the same signal from multiple antenna elements, i.e. the elements of an antenna array. The direction-of-arrival (DOA) of the signal can be estimated based on the phase differences between the elements of the array. So far the reported real-time directional channel measurements have been limited to two dimensions, i.e. the delay and azimuth angle of the signal [1,2]. This kind of measurements typically aim to describe the directional signal environment seen from a base station (BS) of a cellular system. Typically the elevation angle of different incoming signals or multipath components of one signal does not vary significantly at the BS. At the mobile end of the channel, however, the situation can be totally different. For example inside buildings or in street canyons the scatterers close to the mobile cause signal spreading in all three dimensions. The complexity of the realistic environments makes this very difficult to model, and the statistics of the phenomenon are still mostly unknown.

This paper presents a measurement system for directional 3D real-time measurements of the wideband mobile radio channel. The system is based on a spherical antenna array and it enables the complete characterization of the mobile radio channel including time, delay, polarization, and direction in 3D. The measured signal statistics can be used e.g. for developing polarization or pattern diversity antennas for handheld devices. Measurements of realistic radio channels have been performed in various environments: indoor (office building), suburban macrocell, and highway macrocell (array inside a car). Examples of the measured channels are presented in this paper.

2. Description of measurement system

The measurement system is based on a spherical array of 32 dual-polarized antenna elements connected to a complex wideband radio channel sounder via a fast RF switch [3]. The bandwidth of the receiver of the sounder is 100 MHz at carrier frequency of 2154 MHz. The received demodulated signal is divided into I- and Q- branches and sampled with two 120 Ms/s A/D -converters. The signal samples from each branch of the switch are then stored for off line processing to obtain the complex impulse response (IR) of the channel. The number of switched branches is 64, which gives a maximum of 32 antenna elements with two polarizations. The switching is very fast: one impulse response is measured from each of the 64 branches in less than 300 μ s. At normal mobile speeds the channel can be assumed static over this period. Thus, real-time measurements can be made.

Array geometry

The ideal way to cover the whole 4π angle in space with direction-independent angular resolution would be to use equally spaced elements on the surface of a sphere. However, it is not possible to distribute any number of points on a sphere with each one equidistant from its neighbors. In other words, regular polyhedra exists only for certain numbers of vertices. Unfortunately, 32 is not one of them.

The geometry of the built array is based on the dual of the Archimedean solid, the truncated icosahedron, which is probably best known today as the geometry of the football. In this configuration, two different distances between adjacent elements exist. The nearest neighbors of an element are always at a distance of $0.641R$ and the next at $0.714R$ from the element, where R is the radius of the sphere. Each element has either five or six such neighbors. It is shown in [4] that this arrangement minimizes the Coulombic potential of a system of 32 point charges distributed on the surface of a sphere, thus approximating an even distribution.

To reduce cabling and losses, the element switching unit is placed inside the spherical array. Only one signal cable and two control cables are lead out from the array, which minimizes the disturbance in the array radiation. The radius of the built array is $R = 170 \text{ mm}$ (1.22λ at the measurement frequency of 2154 MHz). A smaller radius would result in lower sidelobe level (directional dynamics), but the physical size of the switching unit limits the practically achieved radius.

Array element

The main requirements for the element of the array are two independent orthogonal polarizations with high cross-polarization discrimination, and sufficient bandwidth to meet the requirement of the measurement system. Directive element is also desirable for the spherical array. The geometry of the array element is presented in Figure 1. Figure 2 shows the radiation pattern of the element in both E- and H-planes, measured in the spherical array.

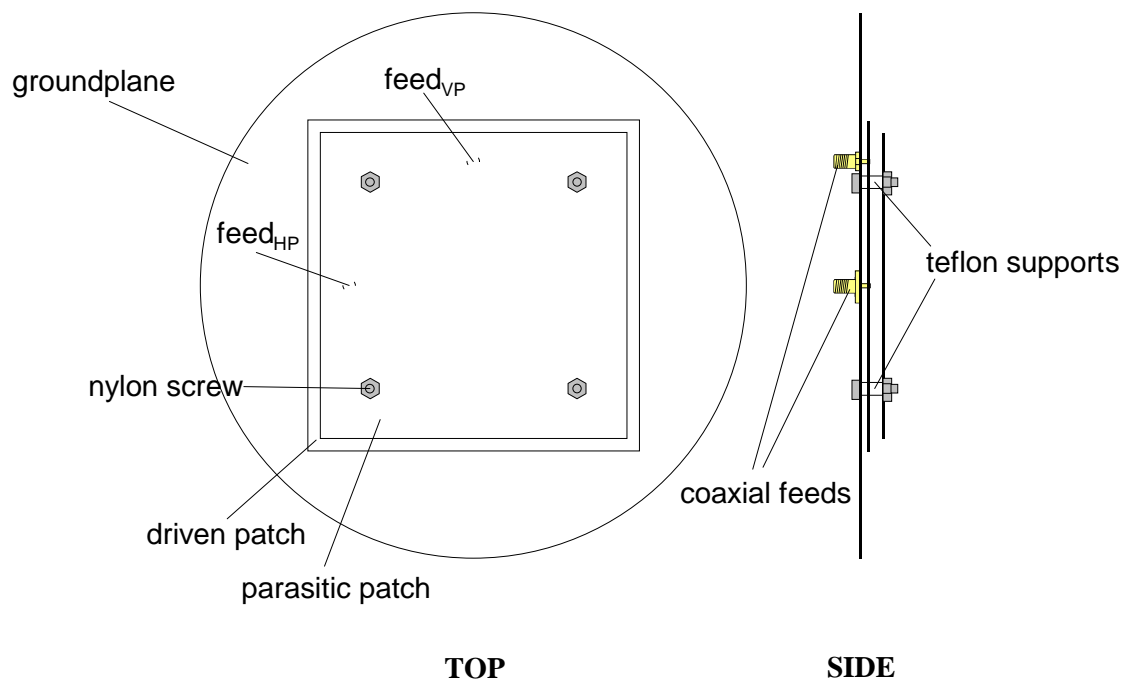


Figure 1. Geometry of the element of the spherical array.

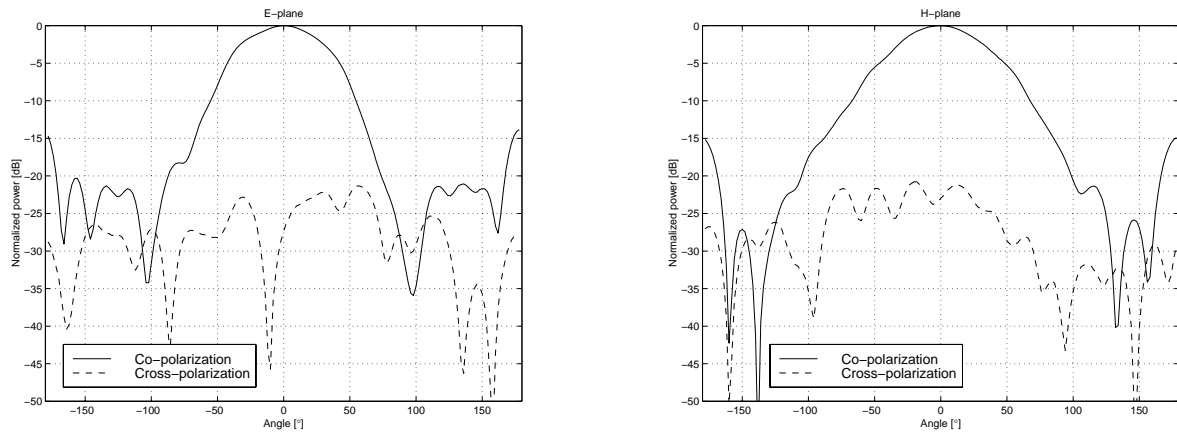


Figure 2. Element radiation pattern measured in the spherical array.

The 6-dB beamwidth of the element is 90° in the E-plane and 100° in the H-plane. The polarization discrimination is better than 18 dB within 6-dB beamwidth. The measured gain of the element is 7.8 dB. The reflection loss is over 10 dB inside the whole measurement band (2.154 ± 0.1 GHz).

Built array

The antenna elements are mounted on a spherical surface consisting of two hollow aluminum hemispheres with outer diameter of 330 mm. The elements are isolated from the mount, and the distance from the center of the fed patch (see Fig. 1.1) to the center of the sphere is 170 mm. The elements point towards the normal of the sphere and they are oriented so that the polarization vectors are parallel to unit vectors \bar{u}_θ and \bar{u}_ϕ . The 64-channel RF switching unit is placed inside the ball together with its control electronics. Only the RF signal cable, two coaxial control cables, and the power supply wires are lead outside the ball. Figure 3 and Figure 4 present the configuration of the spherical array and the switching unit placed inside it.



Figure 3. Spherical array of 32 dual-polarized microstrip patch elements.

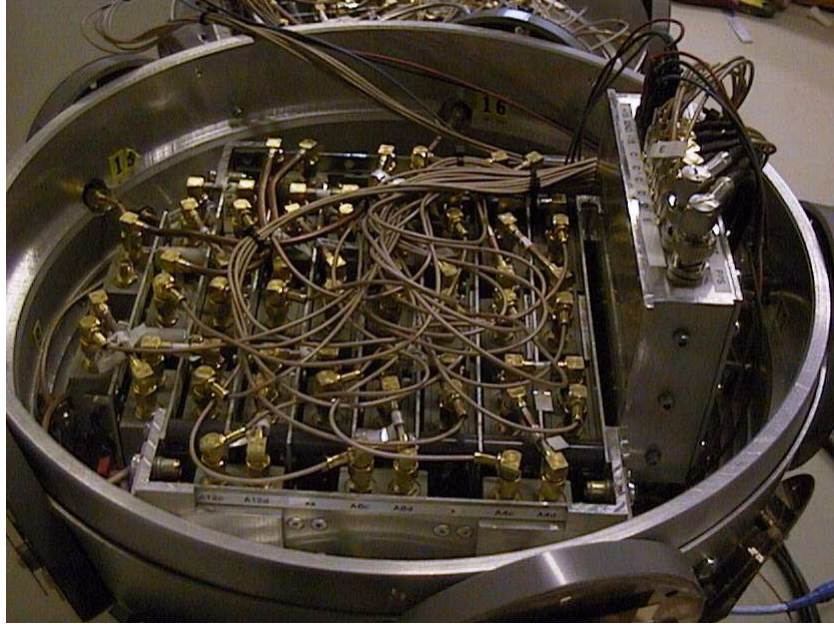


Figure 4. Lower hemisphere of spherical array. Switching unit placed inside the array can be seen.

3. Directional properties of the spherical array

In radio channel sounding, the delay dimension of the channel is solved based on the wideband transmitted signal. The angular dimension, on the other hand, can be computed from the relative phases of the impulse responses measured from different array elements. The resolution and dynamics of the directional measurement depends on the used algorithm as well as the properties of the used antenna array.

The far field of an arbitrary group of antennas at direction (θ, ϕ) can be expressed as

$$\mathbf{E}(\theta, \phi) = q \sum_{n=1}^N w_n e^{j \frac{2\pi}{\lambda} \mathbf{r}_n \cdot \mathbf{u}(\theta, \phi)} \mathbf{g}_n(\theta, \phi) \quad (1)$$

where:

- q = array input signal
- w_n = complex weight of element n
- \mathbf{r}_n = position vector of element n
- $\mathbf{u}(\theta, \phi)$ = unit vector pointing at direction (θ, ϕ)
- $\mathbf{g}_n(\theta, \phi)$ = field pattern of element n

The complex weight vector w can be used to form a beam towards a desired direction. The vector can be found e.g. through numeric beam synthesis [5]. The simplest method is however to phase the elements towards a certain direction (θ_0, ϕ_0) . In this case the weights are written as:

$$w_n(\theta_0, \phi_0) = a_n(\theta_0, \phi_0) e^{-j \frac{2\pi}{\lambda} \mathbf{r}_n \cdot \mathbf{u}(\theta_0, \phi_0)} \quad (2)$$

where a_n is an amplitude tapering coefficient to suppress the sidelobes.

The 3-D angular response of the radio channel can be measured by forming a grid of beams covering the whole 4π solid angle. If s_n is the signal measured from element n at certain polarization, the angular response for that polarization becomes:

$$S(\theta, \phi) = \sum_{n=1}^N w_n(\theta, \phi) s_n, \quad \begin{cases} \theta = -90^\circ \dots +90^\circ \\ \phi = -180^\circ \dots +180^\circ \end{cases} \quad (3)$$

Let us assume a single wave with amplitude q arriving at the array from direction (θ_s, ϕ_s) . In this case signal s_n contains the direction-dependent phase information corresponding to the location of the element, and it is weighted by the element pattern at (θ_s, ϕ_s) :

$$s_n = q e^{j \frac{2\pi}{\lambda} \mathbf{r}_n \cdot \mathbf{u}(\theta_s, \phi_s)} \mathbf{g}_n(\theta_s, \phi_s) \quad (4)$$

Substituting this to Eq. (3) and using element phasing from Eq. (2), gives

$$S(\theta, \phi) = q \sum_{n=1}^N a_n(\theta, \phi) e^{-j \frac{2\pi}{\lambda} \mathbf{r}_n \cdot \mathbf{u}(\theta, \phi) + j \frac{2\pi}{\lambda} \mathbf{r}_n \cdot \mathbf{u}(\theta_s, \phi_s)} \mathbf{g}_n(\theta_s, \phi_s) \quad (5)$$

which is calculated separately for both polarizations. It can be seen that the maximum of the response is produced towards direction $(\theta=\theta_s, \phi=\phi_s)$. The remaining part of the response is not zeros, but spurious responses whose level depends on the geometry of the array, and term a_n . These are equivalent to sidelobes of an antenna array.

The directional properties of the built array have been studied by measuring a known signal environment, using one and two signal sources in an anechoic chamber. Figure 5 and Figure 6 show examples of the directional responses measured in desired polarization in the case of one and two signal sources, respectively. The responses have been calculated using Eq. (3) with weights given in Eq. (2). Exponential amplitude tapering has been applied to suppress the sidelobes. The used tapering function was

$$a_n(\theta, \phi) = \left(\frac{R + \mathbf{r}_n \cdot \mathbf{u}(\theta, \phi)}{2R} \right)^8 \quad (6)$$

where R is the radius of the sphere. The weight of the element pointing at the desired direction is unity while the element pointing at the opposite direction is nulled. Through simulations it has been found that choosing exponent larger than eight does not further suppress the sidelobes. The directional responses are calculated from the peak of the measured impulse response.

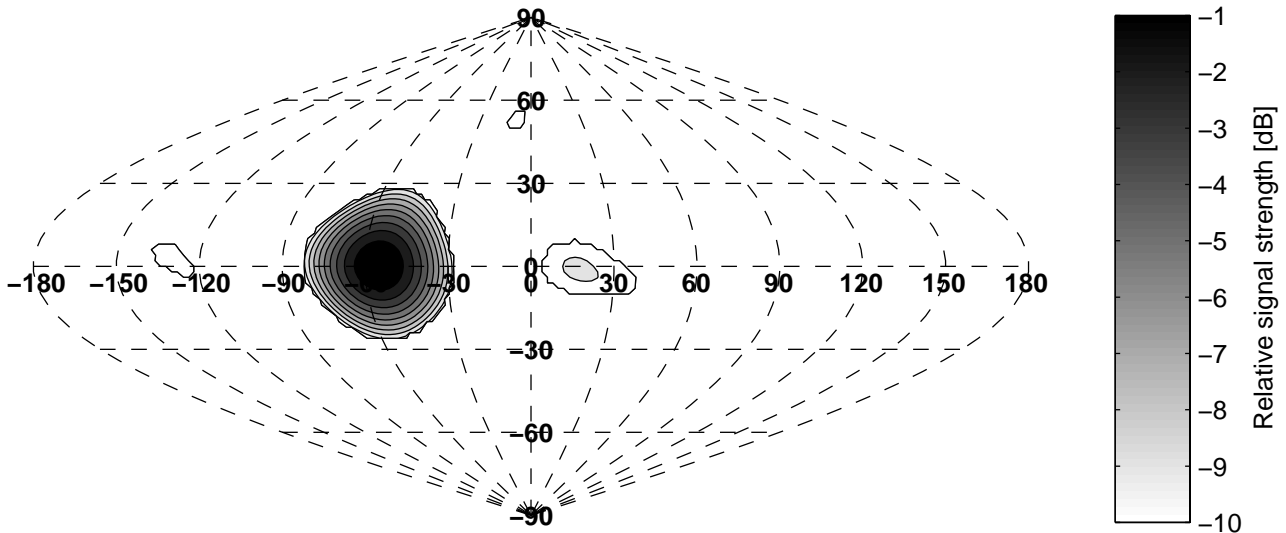


Figure 5. Measured directional response in the case of one signal source. Source in direction $(-58^\circ, 0^\circ)$. Relative levels of $-1 \dots -10$ dB are shown.

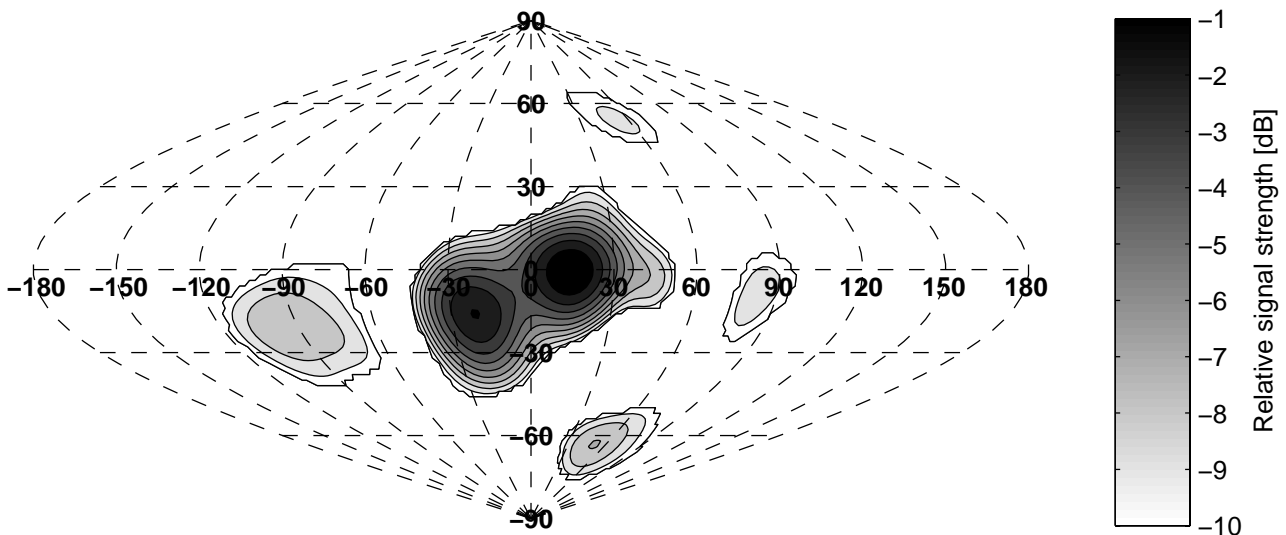


Figure 6. Measured directional response in the case of two signal sources. Sources in directions $(+15^\circ, 0^\circ)$ and $(-16^\circ, -12^\circ)$. Relative levels of $-1 \dots -10$ dB are shown.

In the case of Figure 6 the angular separation of the two sources is approximately 40° , and it can be seen that the sources can be separated at -4 dB level. Therefore we can say that the angular resolution of the array is better than 40° .

The sidelobe level of the array is approximately -9 dB in the case of one signal source, and -7 dB in the case of two signal sources close to each other. The relatively high sidelobe level is due to the oversized array, the maximum distances between elements are 0.9λ . It has to be remembered though, that the sidelobes limit the directional dynamics of the measurement only in the case of multipaths with delay difference smaller than the delay resolution of the measurement (eg. 33 ns with 30 MHz code). Therefore, in most cases the dynamic range of the measurement is determined by the dynamic range of the used spreading code, and typically of the order of 30 dB.

In the cases presented in Figures 5 and 6 the source antenna was vertically polarized, and the responses are calculated using only the θ -polarized element terminals. Due to the small elevation angles of the sources this gives an accurate result, because the orientation of the aperture correspond-

ing to the θ -polarized antenna terminal is almost vertical. However, if the incident angles of the signals were very low or high (signals from down or up), the polarization mismatch would have to be taken into account, and both antenna terminals (θ - and ϕ -polarized) used in the calculation of the directional response to a vertically polarized source.

4. Examples of measured radio channels

Measurements of realistic radio channels have been performed in various environments: indoor (office building), suburban macrocell, and highway macrocell (array inside a car). Examples of the directional channel profiles calculated from the spherical array measurements are presented. The profiles have been calculated from the measured impulse responses using Eqs. (2), (3), and (6).

Example 1: Indoor environment

Figure 7 (a) presents an indoor setup, where the transmitting antenna (BS) was located on the roof of an office building. The receiving array (MS) was inside the building, in a top-floor corridor, 35 m away from the BS. No straight line-of-sight existed, but there was an open door to a room (with windows facing to the BS) at 90° azimuth. The measured impulse response averaged over the elements of the spherical array is shown in Figure 7 (b). The two largest taps that can be identified in the impulse response are marked with vertical dashed lines. The directional profiles calculated for both taps are shown in Figure 8.

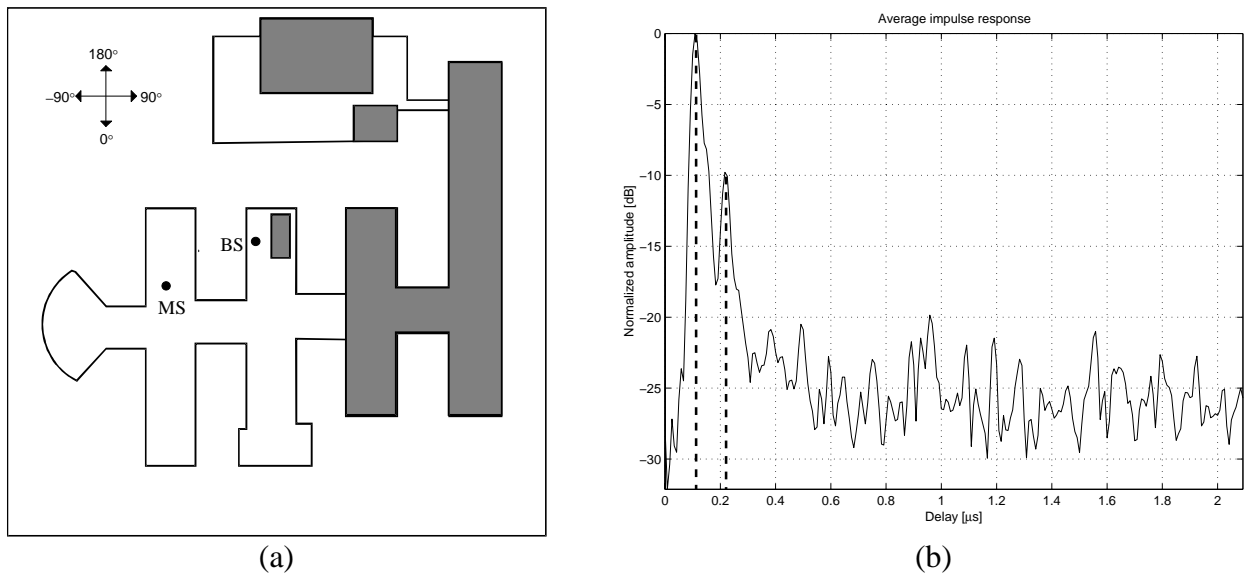


Figure 7. Indoor measurement setup and measured impulse response.

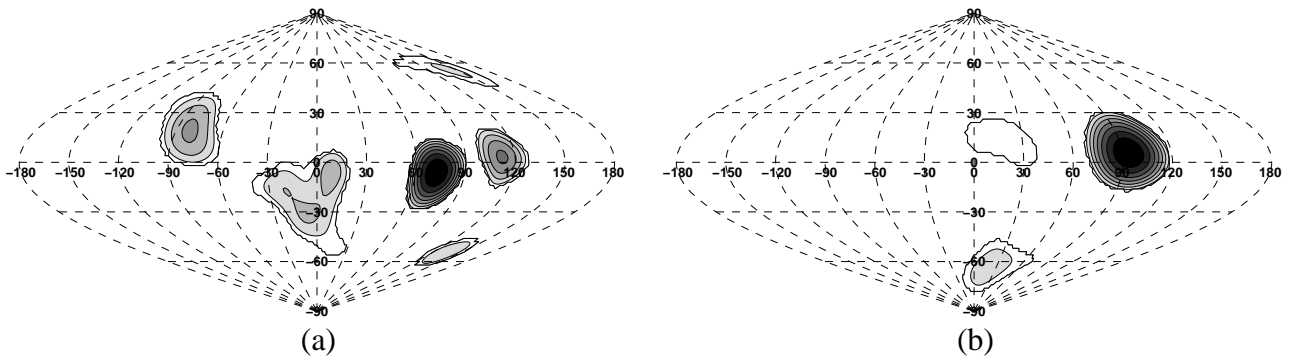


Figure 8. Directional profiles of the taps marked in Figure 7 (b). Relative levels of $-1 \dots -8$ dB are shown. (a) $\tau = 0.11 \mu\text{s}$. (b) $\tau = 0.22 \mu\text{s}$.

It can be seen that the first peak of the impulse response ($\tau = 0.11 \mu\text{s}$) contains actually at least four multipaths. One of them is near to the source direction at $(120^\circ, 7^\circ)$. The second peak at $\tau = 0.22 \mu\text{s}$ is a reflection coming from the direction of the door at 90° azimuth.

Example 2: Suburban macrocell environment

The second example is an outdoor macrocell case with the BS located in a high tower, 50 m above ground. The mobile location was on ground level, on a parking lot next to a 3-storey building, approximately 800 m away from the BS. The environment is suburban with mainly 3-storey buildings. The map of the environment is given in Figure 9 (a). The measured impulse response averaged over the elements of the spherical array is shown in Figure 9 (b). In this case four taps are chosen for angular analysis, and marked with vertical dashed lines. The directional profiles calculated for each tap are shown in Figure 10.

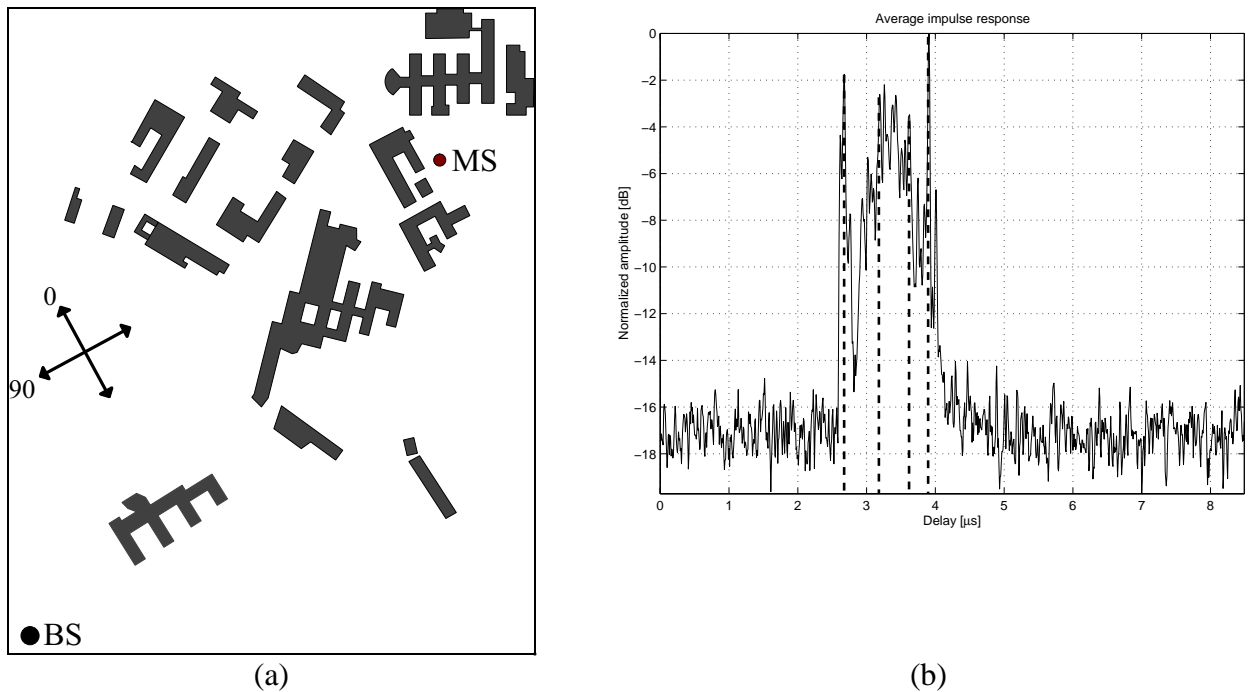


Figure 9. Map of suburban macrocell measurement environment and measured impulse response.

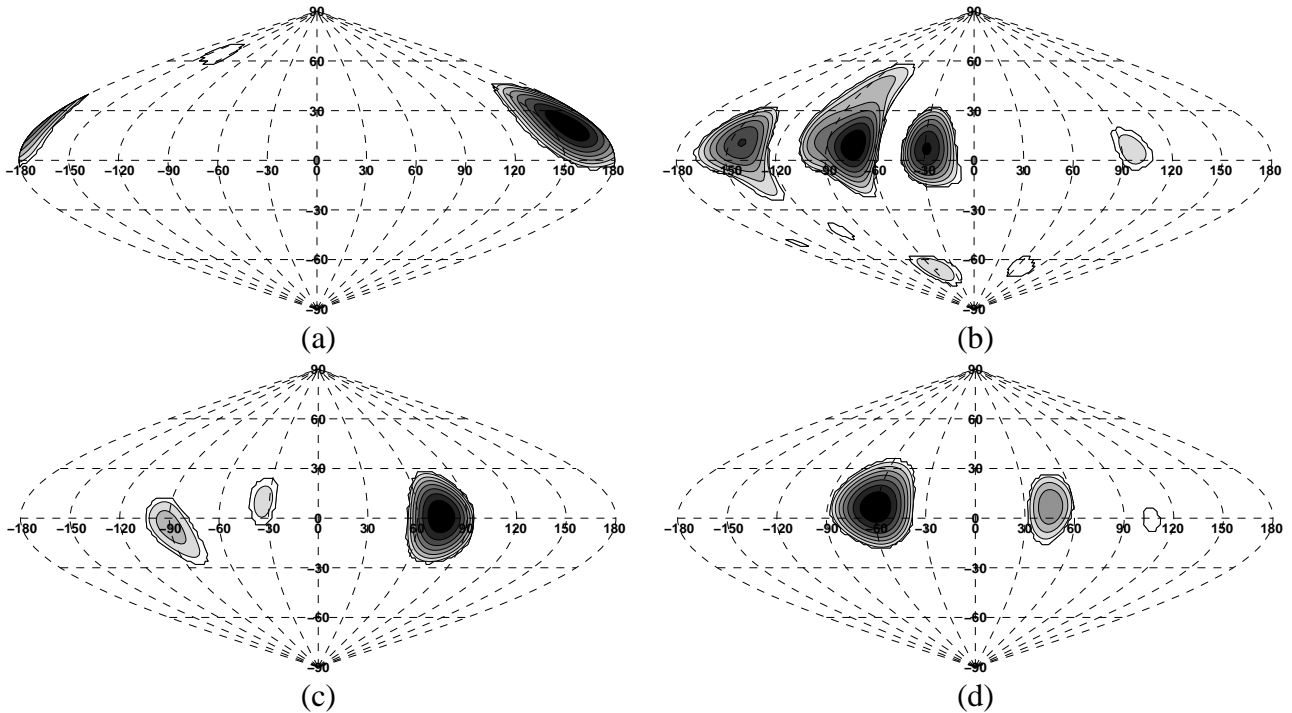


Figure 10. Directional profiles of the taps marked in Figure 9 (b). Relative levels of $-1 \dots -8$ dB are shown. (a) $\tau = 2.7 \mu\text{s}$. (b) $\tau = 3.2 \mu\text{s}$. (c) $\tau = 3.6 \mu\text{s}$. (d) $\tau = 3.9 \mu\text{s}$.

The first multipath ($\tau = 2.7 \mu\text{s}$) is a diffraction from the building corner at 170° azimuth. The elevation angle of 20° is assumed to be caused by the roof-edge of the building. The second tap at $3.2 \mu\text{s}$ contains reflections from the building at around -60° azimuth. The taps at 3.6 and $3.9 \mu\text{s}$ are multiple reflections. If Figure 10 is compared to the indoor profiles of Figure 8, it can be observed that the deviation of the elevation angles is lower in the outdoor case, which is natural due to the more distant reflectors.

5. Conclusions

This paper presents a method for directional 3D real-time measurements of the wideband mobile radio channel. The method is based on a spherical antenna array and it enables the complete characterization of the mobile radio channel including time, delay, polarization, and direction in 3D. The angular resolution of the measurement is approximately 40° , and the dynamic range within one delay tap approximately 9 dB. The measured directional signal statistics can be used e.g. for developing polarization or pattern diversity antennas for handheld devices.

Test measurements of realistic radio channels have been performed in various environments: indoor (office building), suburban macrocell, and highway macrocell (array inside a car). Examples of the measured channels are presented in this paper. More extensive measurement campaigns will be performed in the near future, and the statistical analysis of the measurement results will be made when significant amount of data has been collected.

Acknowledgments

The author wishes to thank Jani Ollikainen and Veli Voipio for helping in the design of the antenna element. Nokia foundation, Wihuri foundation, and Tekniikan edistämisseätiö are gratefully acknowledged for financial support.

References

- [1] K. Kalliola and P. Vainikainen, "Dynamic Wideband Measurement of Mobile Radio Channel with Adaptive Antennas", *Proceedings of 48th IEEE Annual Vehicular Technology Conference*, Ottawa, Ontario, Canada, May 18-21, 1998, pp. 21-25.
- [2] K.I. Pedersen, P.E. Mogensen, and B.H. Fleury, "Spatial Channel Characteristics in Outdoor Environments and their Impact on BS Antenna System Performance", *Proceedings of 48th IEEE Annual Vehicular Technology Conference*, Ottawa, Ontario, Canada, May 18-21, 1998, pp. 719-723.
- [3] K. Kalliola and P. Vainikainen, "Characterization System for Radio Channel of Adaptive Array Antennas", *Proceedings of 8th IEEE International Symposium on Personal, Indoor and Mobile Radio Communications*, Helsinki, Finland, September 1-4 1997, pp. 95-99.
- [4] J.R. Edmundson, "The Distribution of Point Charges on the Surface of a Sphere", *Acta Crystallographica*, A48, 1992, pp. 60-69.
- [5] L.I. Vaskelainen, "Iterative Least-Squares Synthesis Methods for Conformal Array Antennas with Optimized Polarization and Frequency Properties", *IEEE Transactions on Antennas and Propagation*, Vol. AP-45, July 1997, pp. 1179-1185.